available at www.sciencedirect.com

ScienceDirect

journal homepage: www.elsevier.com/locate/carbon

Neutralized fluorine radical detection using single-walled carbon nanotube network

Sehun Jung[a], *Seunghyun Hong*[b], *Byoungjae Park*[c], *Jaeboong Choi*[a], *Youngjin Kim*[a,b], *Geunyoung Yeom*[b,c], *Seunghyun Baik*[a,b,*]

[a]*School of Mechanical Engineering, Sungkyunkwan University, Suwon 440-746, Republic of Korea*
[b]*SKKU Advanced Institute of Nanotechnology (SAINT), Sungkyunkwan University, Suwon 440-746, Republic of Korea*
[c]*Department of Materials Science and Engineering, Sungkyunkwan University, Suwon 440-746, Republic of Korea*

ARTICLE INFO

Article history:
Received 28 June 2007
Accepted 19 October 2007
Available online 26 October 2007

ABSTRACT

It is known that single-walled carbon nanotubes (SWCNTs) can be functionalized by fluorine gas. Here, we report neutralized fluorine radical detection using a matted sheet of SWCNTs, prepared by alternating current dielectrophoresis. Upon exposure to neutralized radicals containing fluorine atoms in a plasma, as model analytes, the conductance of the SWCNT matt showed fast modulation. The transduction mechanism was investigated by electrical transport measurements, X-ray photoelectron spectroscopy and Raman spectroscopy. Metallic nanotubes were shown to react covalently to the near exclusion of semiconducting species. The selectivity was promoted by the curvature-induced strain of the nanotubes. The results open new opportunities for the detection of fluorine radicals at specific locations inside the reaction zone using a simple, miniaturized carbon nanotube network.

1. Introduction

The unique electronic, optical and structural properties of carbon nanotubes enable a wide range of applications [1–3] including biosensors [4–6] and chemical sensors [7,8]. Especially, single-walled carbon nanotubes (SWCNTs) have optimal characteristics as sensor elements such as large surface-to-volume ratios, one-dimensional electronic structure and a molecular composition consisting of only surface atoms [9]. SWCNTs have been utilized to detect gases and organic vapors, at analyte concentrations well below the ppm level, including oxygen, NO_2, NH_3 and nerve agent simulants [7,8,10].

The identification and quantification of reactive radicals has become increasingly important for physicists and chemists [11]. In most cases, the information of radicals is not sufficiently characterized in reaction processes including plasma-based surface treatments, which have been widely used for industries. Raman [12], fluorescence [13], absorption [14] and mass [11] spectroscopic techniques have been employed to detect radicals, which need expensive equipments. Besides, these techniques are difficult to provide information at specific locations inside the reaction zone without perturbing the system. Recently, electrical and chemical response of nanotubes upon exposure to CH_4 and H_2 plasma has been investigated [15,16].

In this work, we demonstrated fast conductance modulation of the SWCNT matt in response to neutralized radicals containing fluorine atoms where the functionalization of metallic nanotubes dominated the transport behavior. The SF_6 gas was dissociated into electrons, ions, radicals and stable products in an RF plasma chamber, and the neutralized

* *Corresponding author:* Address: School of Mechanical Engineering, Sungkyunkwan University, Suwon 440-746, Republic of Korea. Fax: +82 31 290 5889.
E-mail address: sbaik@me.skku.ac.kr (S. Baik).
0008-6223/$ - see front matter
doi:10.1016/j.carbon.2007.10.019

radical beam was generated using a three-grid ion gun and a reflector to minimize the effects from charged ions and electrons.

2. Experimental

Anionic surfactant sodium dodecyl sulfate (SDS) was used to suspend HiPco-SWCNTs according to a previously published protocol [1]. Thirty milligrams of HiPco-SWCNTs (purchased from Carbon Nanotechnologies Inc.) was dispersed in 100 mL of aqueous SDS solution (1 wt% in deionized water) by 1 h of homogenization at a power level of 4 W (Taitec VP-5S). The mixed solution was then ultrasonicated for 15 min at 490 W (Ulsso Hi-Tech 7005). Subsequently, the sample was centrifuged (Beckman Coulter LE-80K) for 4 h at 170,000 g (22,600 rpm) to remove aggregated SWCNTs, and the upper supernatant was immediately decanted. Finally, the decanted SWCNT solution was diluted using aqueous SDS solution (1 wt%), resulting in a nanotube mass concentration of 10 mg/L.

A matted sheet of SWCNTs was formed on a p-type (100) silicon wafer with a thermally coated 500-nm-thick oxide layer. As shown in Fig. 1a, microelectrodes with a gap size of 5 μm were fabricated using a conventional photolithographic method. A 5-nm-thick titanium (Ti) and a 200-nm-thick gold (Au) were thermally deposited on the SiO_2 layer to form electrical contacts. Subsequently, microelectrodes were wired (Kulicke & Soffa 4524) to a chip carrier (Global Chip Materials SB2438001). A matted sheet of SWCNTs was deposited on the electrodes using alternating current dielectrophoresis [17–19]. A drop of HiPco-SWCNTs (10 mg/L, 20 μL) was placed on the electrode after applying alternating current at a frequency of 10 MHz and a peak-to-peak voltage of 10 V using a function generator (Agilent 33220A). After a delay of 10 min, the droplet was blown off by a stream of nitrogen gas, and the function generator was switched off. We previously demonstrated the presence of both metallic and semiconducting nanotubes when the dielectrophoretic deposition was carried out using ionic surfactant micellized SWCNTs [18,19].

The SWCNT network was exposed to neutralized radicals created in SF_6 plasma. SF_6 is a commonly used etching gas which serves as a source of radicals containing fluorine atoms for etching polycrystalline silicon [20]. The SF_6 gas molecules were dissociated into electrons (e^-), ions (SF_3^+, SF_5^+, SF_2^+, SF^+, F^+, S_2F^+, S^+, SF_6^-, SF_5^-, SF_4^-, etc.), radicals (SF_5, SF_3, SF, F, S, etc.) and stable products (SF_4, SF_2, F_2, etc.) in a plasma [21–27]. The predominant species were SF_3^+, SF_5^+, SF_2^+, SF^+ ions, SF_5, SF_3, SF radicals, and SF_2, F_2 stable products [28].

In order to minimize the effects of ions and electrons on nanotubes, a low-angle forward-reflected neutral beam source was generated using a three-grid ion gun and a reflector with a conversion efficiency of 99.7%, as shown in Fig. 1b [28]. The plasma chamber was pumped down to a vacuum pressure of 0.0013 Pa, and SF_6 gas (99.999%) was introduced (10 sccm, 0.13 Pa). The SF_6 gas molecules were dissociated into electrons, ions, radicals and stable products when the power (200 W) was applied at a radio frequency of 13.56 MHz. The ions from the plasma source were extracted

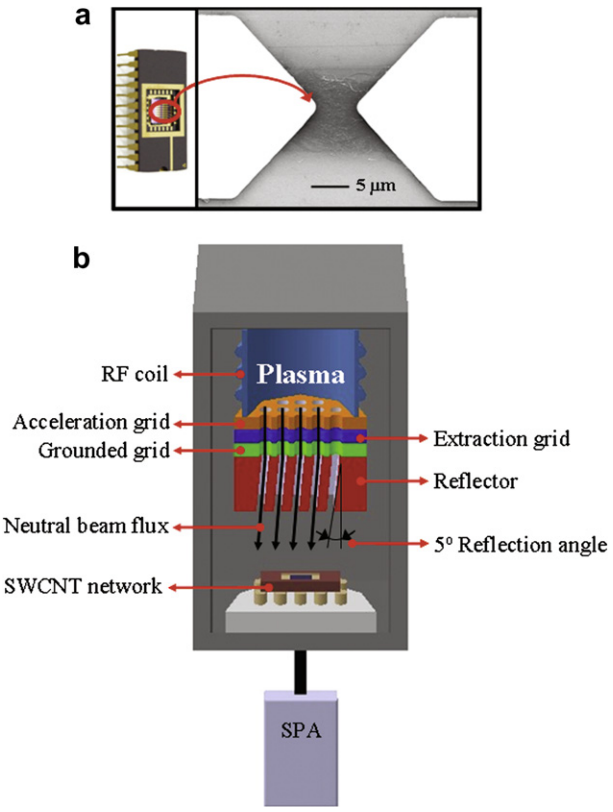

Fig. 1 – Experimental setup. (a) Microelectrodes wired to a chip carrier. SEM image of dielectrophoretically deposited nanotubes at the 5 μm electrode gap is magnified. (b) A schematic diagram of the plasma chamber. The SF_6 plasma was generated by RF power. A three-grid ion gun and a low angle (5°) forward reflector were used to extract neutralized radical beam source. The SWCNT network was directly connected to a semiconductor parameter analyzer.

by applying 100 V, −400 V and 0 V to the 1st acceleration grid, 2nd extraction grid and 3rd grounded grid, respectively. The extracted ions were reflected on a flat surface (reflector) to produce neutralized radical beam flux. The non-neutralized ion flux (0.3%), measured using a Faraday cup, was 1.2 μA/cm^2. The neutralized radical flux was estimated to be $1.646 \times 10^{16}/cm^2$ s, calculated using the experimentally determined ion flux and the theoretically obtained relative reaction rates of ions and radicals of the SF_6 gas in a plasma [21]. We previously characterized radical peaks such as F_2, SF, SF_2, SF_3 and SF_5 in the neutral beam using a quadrupole mass spectrometer [28].

The SWCNT network was placed at 30 cm away from the reflector, and the conductance modulation was real-time monitored using a semiconductor parameter analyzer (Agilent E5262A). In addition, the electrical transport characteristics of the SWCNT network were analyzed before and after the exposure process to investigate the transduction mechanism using a semiconductor parameter analyzer (Agilent E5262A) and a probe station (CASCADE RF-1). The source–drain current at a source–drain voltage of 1 V was monitored as a function of the back gate voltage. Raman spectra before and after the exposure were analyzed using a Raman

microscope (Renishaw, inVia Reflex). A HeNe laser with a grating of 1800 grooves/mm was used for 632.8 nm excitation. The laser power at the sample was 20 mW, and the spot size was 1–2 μm in diameter. Also, the X-ray photoelectron spectroscopy (XPS; ESCA 2000) was carried out to investigate chemical species attached to SWCNTs using Al Kα (1486.6 eV) at 200 W with a pass energy of 20 eV.

3. Results and discussion

Fig. 2a shows real-time kinetics of the SWCNT network during the exposure process. The chamber was pumped down to a vacuum pressure of 0.0013 Pa, and SF_6 gas was supplied at 100 s (10 sccm, 0.13 Pa). The current through the SWCNT matt did not respond to the SF_6 gas. The source–drain voltage was 1 V. The RF power was turned on at 400 s. The current immediately decreased upon exposure to radicals containing fluorine atoms, reaching zero at 697 s. This clearly indicated that the nanotube network responded to fluorine radicals rather than pure SF_6 gas. The RF power was turned off at 800 s. Cycling to pure SF_6 gas did not recover conductance, demonstrating that the radicals were irreversibly chemisorbed onto the surface of SWCNTs.

Fig. 2b shows the normalized F 1s spectra of the SWCNT network before and after the exposure. Three different forms of C–F bonds were revealed by de-convoluting the F 1s spectra of the fluorine radical exposed nanotubes with Gaussian peaks. A large covalent C–F bond (687.5 eV) and a small semi-ionic C–F bond (685.5 eV) were observed [29,30]. Also, a third peak at 689.2 eV was detected, possibly due to the presence of p-(CF_2=CF_2) bond [31]. These observations indicated that fluorine radicals took a major role in the reaction with carbon nanotubes. Sulfur itself is known not to interact with nanotubes [32], and the peak related with sulfur was not observed. The XPS data were similar to those found by exposing nanotubes to fluorine gas [33] and CF_4 plasma [34,35]. The development of the fluorinated carbon bonds was proposed to be caused by the strongly increased localization of pi electrons of C atoms as a result of the increased F density [33,34].

Fig. 2c shows the source–drain current (I) measured as a function of the back gate voltage (V_G) at room temperature. In these data sets, the exposure process was stopped right before reaching zero source–drain current, at $V_G = 0$, in order to investigate responses of both metallic and semiconducting nanotubes. Before the exposure, electrical transport characteristics exhibited both conduction (28.4 μA) at a positive gate voltage of 30 V and modulation of the current with changing gate voltage. This observation was consistent with a mixture of metallic and semiconducting pathways [18]. The increment in current with decreasing gate voltage, $\Delta I_{\text{before exposure}}$ = 2.2 μA, was attributed to the transport through p-type semiconducting species [7,36]. The current at $V_G = 30$ V significantly decreased upon exposure to radicals containing fluorine atoms whereas the increment showed slight difference ($\Delta I_{\text{after exposure}}$ = 1.7 μA). This indicated that metallic species were preferentially reacted to the near exclusion of semiconducting SWCNTs. Yang et al. also showed selective suppression of metallicity of a SWCNT matt by exposing it to fluorine gas for 30 min at 0.1 bar and room temperature [33].

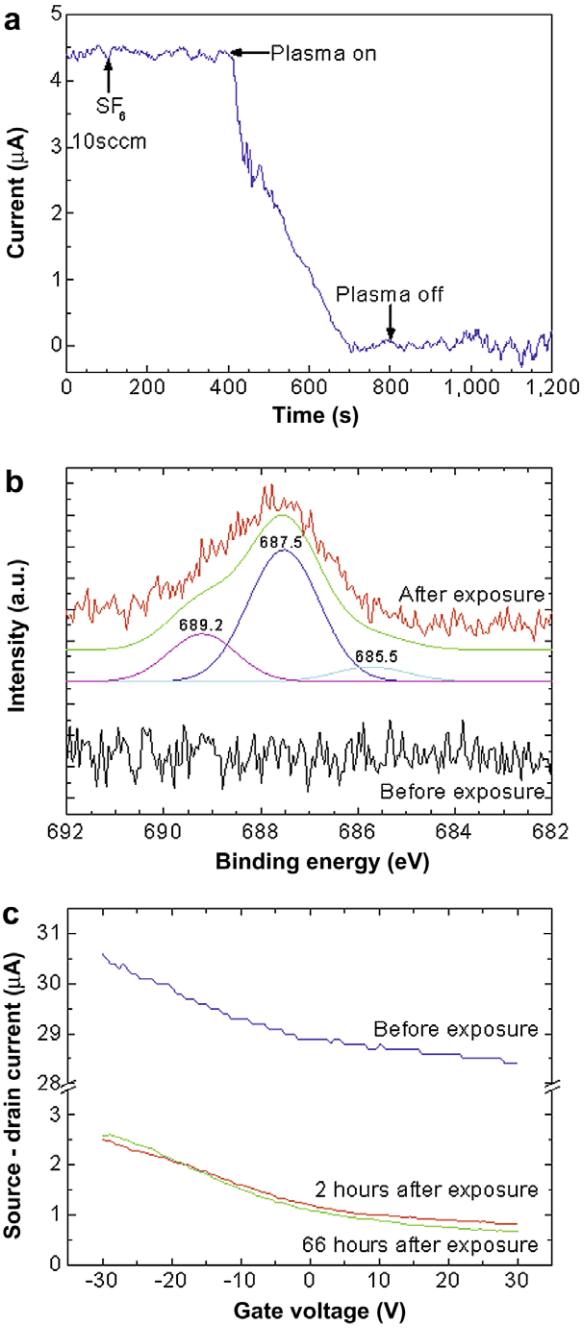

Fig. 2 – Investigating the mechanism of signal transduction. (a) Transient response of the SWCNT network upon exposure to radicals containing fluorine atoms. The SF_6 gas was supplied at 100 s. The RF power was applied between 400 s and 800 s. Source–drain voltage was 1 V. (b) XPS spectra of F 1 s peaks of the SWCNT network before and after the exposure. (c) Source–drain current as a function of the back gate voltage. The measurements were carried out right before, 2 h after and 66 h after the exposure. Source–drain voltage was 1 V.

The F–F bond became weak as the gas approached nanotubes. Consequently, the C–F bond formed on the sidewall of nanotubes. Large charge transfer was expected from metallic

species due to more abundant pi electron density at the Fermi level compared with semiconducting SWCNTs, leading to the lower adsorption barrier height and easier accessibility for metallic SWCNTs [33]. It is interesting to note that the response of the SWCNT network to fluorinated radicals was much faster than the response to fluorine gas [33] or solution-based functionalizing reagents [37] probably due to the vigorous reactivity of radicals. The measurement carried out at 66 h after the exposure showed little difference. This observation confirmed the irreversibly chemisorbed fluorinated species.

Scanning electron microscopy images of the nanotube device before and after the exposure to fluorine radicals do not show apparent destruction of the nanotube structure under the current experimental conditions (Fig. 3). However, more detailed studies using transmission electron microscopy need to be carried out to investigate modification of the tubular structure.

As shown in Fig. 4, Raman spectroscopic observations further supported the findings from XPS and electrical transport measurements. Fig. 4a shows Raman spectra of the SWCNT matt before and after the exposure to radicals containing fluorine atoms. The phonon mode at 1330 cm^{-1}, also known as the D mode, corresponds to the conversion of an SP^2 C to an SP^3 C on the nanotube, indicating the extent of sidewall functionalization [37,38]. The G′ band at 2700 cm^{-1} is an overtone of the D band [38]. The increased intensity ratios of the D/G and D/G′ bands indicated covalent functionalization by the fluorine radicals (Fig. 4b), which was consistent with the XPS and electrical transport observations.

Fig. 4c shows radial breathing mode spectra, and chiral vectors for metallic nanotubes are shown in bold italics. The functionalization to the sidewall of the nanotube decreases the resonantly enhanced, low frequency Raman mode that is distinct for the particular (n,m) nanotube [37]. At 632.8 nm excitation, both metallic and semiconducting types are in resonance for the HiPco material. The peaks for metallic SWCNTs were relatively suppressed with the reaction compared with those of semiconducting types, supporting the I–V_G measurements shown in Fig. 2c. Fig. 4d compares the intensity ratios of (12,3)/(10,3) and (13,4)/(10,3) chiral peaks. The diameters of (13,4), (12,3) and (10,3) nanotubes are 1.205 nm, 1.1 nm and 0.923 nm, respectively. The intensity ratio of (12,3)/(10,3) significantly decreased after the exposure to radicals containing fluorine atoms whereas that of (13,4)/(10,3) slightly decreased. Yang et al. also observed diameter dependent selective removal of metallic SWCNTs using fluorine gas [33]. The selectivity became less obvious for the nanotubes with larger diameters, indicating that the selective functionalization was promoted by curvature-induced strain.

The simple, miniaturized SWCNT matt showed sensitive response upon exposure to neutralized fluorine radicals. Experimental investigations carried out by electrical transport measurements, XPS and Raman spectroscopy suggested that metallic carbon nanotubes were covalently functionalized with fluorine radicals. However, regeneration and selectivity issues remain to be addressed. Therefore, we propose to use the SWCNT network for applications where these issues are insignificant. For example, the detection of dissociation of a specific type of gas inside a closed system, such as a plasma chamber, does not involve the selectivity issue since the introduced gas type is known. Another practical application could be the detection of dissociation of SF_6 gas in gas-insulated switchgears (GIS) due to partial discharge [39]. SF_6 gas is widely used as electrical insulator as well as arc-quenching medium in high-power electrical devices such as GIS. Partial discharge due to the intensified electric field leads to dissociation of the insulating gas (SF_6), which degrades the performance of GIS. In this case, regeneration is not an important factor since the dissociated SF_6 gas in a closed chamber is not regenerated. Therefore, the accumulative nature of covalent bonding is appropriate for this type of application. Eventually, the insulating gas and the SWCNT network, which can be fabricated at a low cost, need to be replaced if the degree of dissociation of SF_6 gas exceeds over a certain standard. Also, the selectivity issue is not important since the dissociation pattern of SF_6 gas is known.

More detailed experiments at different plasma powers and SF_6 flow rates need to be carried out to experimentally determine the detection limit of the SWCNT network. Previous experimental investigations demonstrated that SWCNT-based chemical sensors could detect gaseous analytes at concentrations well below the ppm level [7,8,10]. Therefore, the SWCNT network would detect fluorine radicals with high sensitivity. Besides, investigations using an isolated single-walled carbon nanotube device might provide improved sensitivity and more insight about the mechanism.

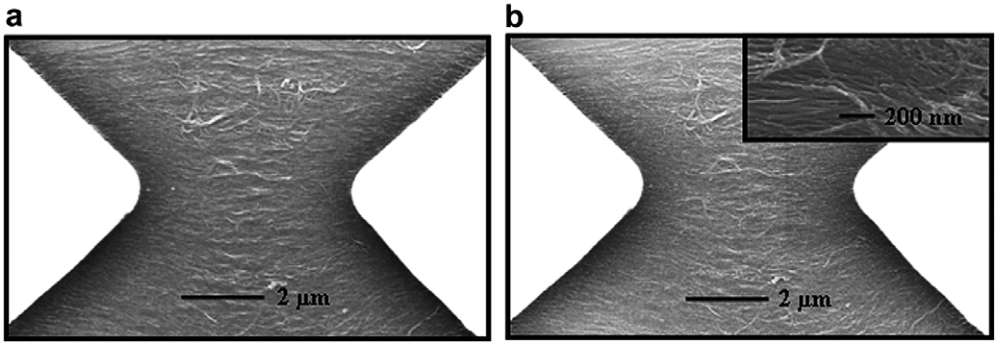

Fig. 3 – SEM images of the nanotube device before (a) and after (b) the exposure to fluorine radicals. The inset provides the magnified image of SWCNT matt.

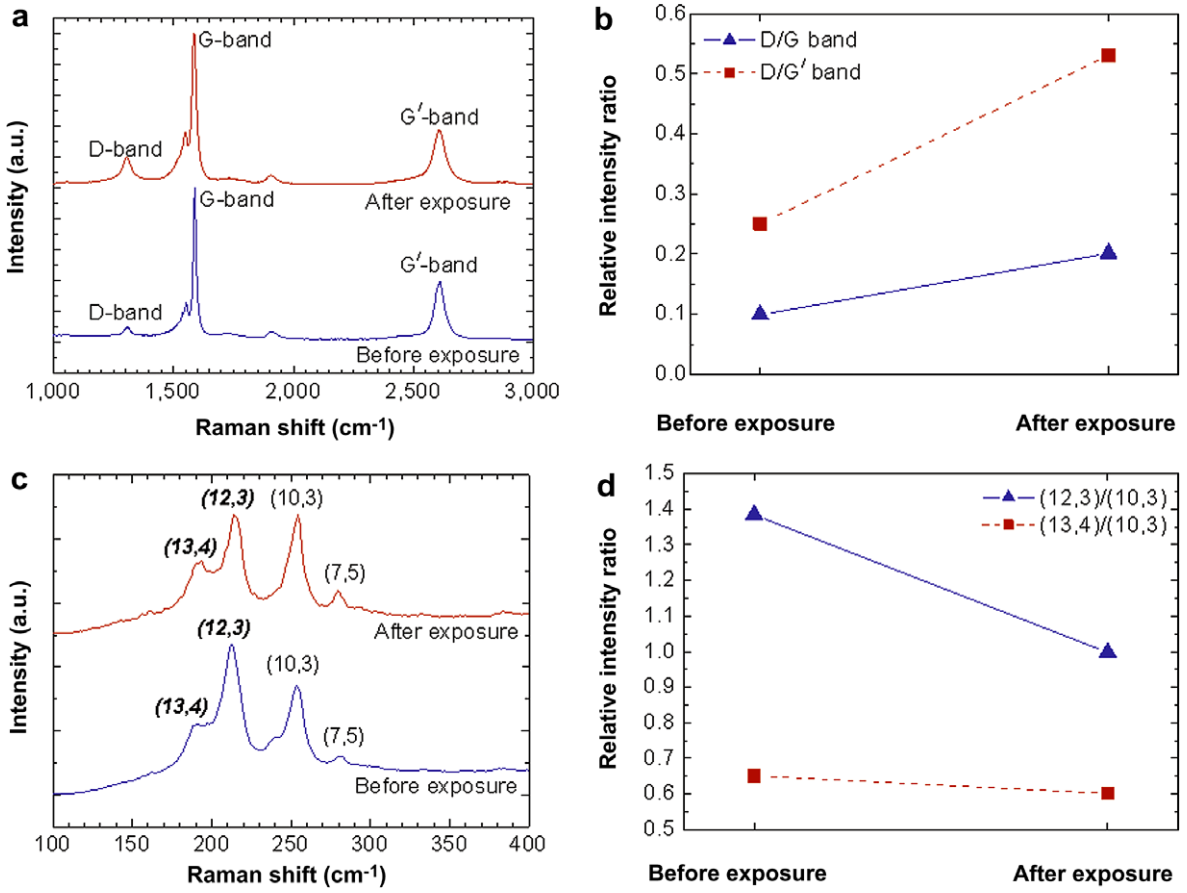

Fig. 4 – Raman spectroscopic observations at 632.8 nm excitation. (a) Raman spectra of the SWCNT network before and after the exposure to radicals containing fluorine atoms. (b) Relative intensity ratios of D/G and D/G′ bands. (c) Radial breathing modes showed the selective suppression of metallicity of the SWCNT network. (d) Relative intensity ratios of (12,3)/(10,3) and (13,4)/(10,3) nanotubes.

4. Conclusion

In summary, the matted sheet of SWCNTs could provide fast identification of radicals containing fluorine atoms. The mechanism was based on the preferential chemisorption of the neutralized fluorine radicals onto smaller diameter metallic nanotubes, which was proved by electrical transport measurements, XPS and Raman spectroscopy. The SWCNT network can be used to detect reactive radicals at specific locations inside the reaction zone due to the simple, miniaturized nature. Cross-checking experiments at different RF powers and gas flow rates, using both laser spectroscopic techniques and SWCNT networks, would provide more accurate quantification of radicals. Also, the sensitivity might be improved by employing a single, small diameter metallic nanotube.

Acknowledgement

This work has been supported by KESRI (R-2007-2-061), which is funded by MOCIE (Ministry of commerce, industry and energy).

REFERENCES

[1] O'Connell MJ, Bachilo SM, Huffman CB, Moore VC, Strano MS, Haroz EH, et al. Band gap fluorescence from individual single-walled carbon nanotubes. Science 2002;297:593–6.
[2] Bachilo SM, Strano MS, Kittrell C, Hauge RH, Smalley RE, Weisman RB. Structure-assigned optical spectra of single-walled carbon nanotubes. Science 2002;298:2361–6.
[3] Iijima S. Helical microtubules of graphitic carbon. Nature 1991;354:56–8.
[4] Barone PW, Baik S, Heller DA, Strano MS. Near-infrared optical sensors based on single-walled carbon nanotubes. Nat Mater 2005;4:86–92.
[5] Hwang ES, Cao C, Hong S, Jung HJ, Cha CY, Choi JB, et al. The DNA hybridization assay using single-walled carbon nanotubes as ultrasensitive, long-term optical labels. Nanotechnology 2006;17:3442–5.
[6] Kam NWS, Jessop TC, Wender PA, Dai H. Nanotube molecular transporters: internalization of carbon nanotube-protein conjugates into mammalian cells. J Am Chem Soc 2004;126:6850–1.
[7] Kong J, Franklin NR, Zhou C, Chapline MG, Peng S, Cho K, et al. Nanotube molecular wires as chemical sensors. Science 2000;287:622–5.

[8] Collins PG, Bradley K, Ishigami M, Zettl A. Extreme oxygen sensitivity of electronic properties of carbon nanotubes. Science 2000;287:1801–4.
[9] Lee CY, Strano MS. Understanding the dynamics of signal transduction for adsorption of gases and vapors on carbon nanotube sensors. Langmuir 2005;21:5192–6.
[10] Lee CY, Baik S, Zhang J, Masel RI, Strano MS. Charge transfer from metallic single-walled carbon nanotube sensor arrays. J Phys Chem B 2006;110:11055–61.
[11] Kang HD, Dose V. Radical detection in a methane plasma. J Vac Sci Technol A 2003;21:1978–80.
[12] Hay SO, Roman WC, Colket MB. CVD diamond deposition processes investigation: CARS diagnostics/modeling. J Mater Res 1990;5:2387–97.
[13] Hancock G, Sucksmith JP, Toogood MJ. Plasma kinetic measurements using time-resolved actinometry: comparisons with laser-induced fluorescence. J Phys Chem 1990;94:3269–72.
[14] Haverlag M, Stoffels E, Stoffels WW, Kroesen GMW, de Hoog FJ. Measurements of radical densities in radio-frequency fluorocarbon plasmas using infrared absorption spectroscopy. J Vac Sci Technol A 1994;12:3102–8.
[15] Zhang G, Qi P, Wang X, Lu Y, Li X, Tu R, et al. Selective etching of metallic carbon nanotubes by gas-phase reaction. Science 2006;314:974–7.
[16] Zhang G, Qi P, Wang X, Lu Y, Mann D, Li X, et al. Hydrogenation and hydrocarbonation and etching of single-walled carbon nanotubes. J Am Chem Soc 2006;128:6026–7.
[17] Krupke R, Hennrich F, Lohneysen H, Kappes MM. Separation of metallic from semiconducting single-walled carbon nanotubes. Science 2003;301:344–7.
[18] Baik S, Usrey M, Rotkina L, Strano MS. Using the selective functionalization of metallic single-walled carbon nanotubes to control dielectrophoretic mobility. J Phys Chem B 2004;108:15560–4.
[19] Kim Y, Hong S, Jung S, Strano MS, Choi J, Baik S. Dielectrophoresis of surface conductance modulated single-walled carbon nanotubes using catanionic surfactants. J Phys Chem B 2006;110:1541–5.
[20] Sun HC, Whittaker EA. Real-time in situ detection of SF_6 in a plasma reactor. Appl Phys Lett 1993;63:1035–7.
[21] Riccardi C, Barni R, De Colle F, Fontanesi M. Modeling and diagnostic of an SF_6 RF plasma at low pressure. IEEE Trans Plasma Sci 2000;28:278–87.
[22] Brand KP, Jungblut H. The interaction potentials of SF_6 ions in SF_6 parent gas determined from mobility data. J Chem Phys 1983;78:1999–2007.
[23] Anderson HM, Merson JA, Light RW. A kinetic model for plasma etching in a SF_6/O_2 RF discharge. IEEE Trans Plasma Sci 1986;14:156–64.
[24] Wagner JJ, Brandt WW. DC plasma etching of silicon by SF_6, mass spectroscopic study of the discharge products. Plasma Chem Plasma Process 1981;1:201–15.
[25] Foest R, Olthoff JK, Van Brunt RJ, Benck EC, Roberts JR. Optical and mass spectrometric investigations of ions and neutral species in SF_6 radio-frequency discharges. Phys Rev E 1996;54:1876–87.
[26] Turban G, Coulon JF, Mutsukura N. A mechanistic study of SF_6 reactive ion etching of tungsten. Thin Solid Films 1989;176:289–308.
[27] Nagaseki K, Kobayashi H, Ishikawa I, Nishimura E, Saito Y, Suganomata S. Mass spectrometry of discharge products at 13.56 MHz in SF_6 gas. Jpn J Appl Phys Part 1 1994;33:4348–52.
[28] Chung MJ, Lee DH, Yeom GY. Diagnostics of neutral species in the low-angle forward-reflected neutral beam etching system. Surf Coat Technol 2003;171:231–6.
[29] Jiang L, Cheung R, Brown R, Mount A. Inductively coupled plasma etching of SiC in SF_6/O_2 and etch-induced surface chemical bonding modifications. J Appl Phys 2003;93:1376–83.
[30] Nanse G, Papirer E, Fioux P, Moguet F, Tressaud A. Fluorination of carbon blacks: an X-ray photoelectron spectroscopy study: I. A literature review of XPS studies of fluorinated carbons. XPS investigation of some reference compounds. Carbon 1997;35:175–94.
[31] Moulder JF, Stickle WF, Sobol PE, Bomben KD. Handbook of X-ray Photoelectron Spectroscopy. Minnesota: Perkin–Elmer; 1993. p. 46–7.
[32] Goldoni A, Petaccia L, Gregoratti L, Kaulich B, Barinov A, Lizzit S, et al. Spectroscopic characterization of contaminants and interaction with gases in single-walled carbon nanotubes. Carbon 2004;42:2099–112.
[33] Yang CM, An KH, Park JS, Park KA, Lim SC, Cho SH, et al. Preferential etching of metallic single-walled carbon nanotubes with small diameter by fluorine gas. Phys Rev B 2006;73:075419/1–7.
[34] Plank NOV, Jiang L, Cheung R. Fluorination of carbon nanotubes in CF_4 plasma. Appl Phys Lett 2003;83:2426–8.
[35] Felten A, Bittencourt C, Pireaux JJ, Van Lier G, Charlier JC. Radio-frequency plasma functionalization of carbon nanotubes surface O_2, NH_3 and CF_4 treatments. J Appl Phys 2005;98:074308/1–9.
[36] Martel R, Schmidt T, Shea HR, Hertel T, Avouris P. Single- and multi-wall carbon nanotube field-effect transistors. Appl Phys Lett 1998;73:2447–9.
[37] Strano MS, Dyke CA, Usrey ML, Barone PW, Allen MJ, Shan H, et al. Electronic structure control of single-walled carbon nanotube functionalization. Science 2003;301:1519–22.
[38] Dresselhaus MS, Dresselhaus G, Saito R, Jorio A. Raman spectroscopy of carbon nanotubes. Phys Rep 2005;409:47–99.
[39] Suehiro J, Zhou G, Hara M. Detection of partial discharge in SF_6 gas using a carbon nanotube-based gas sensor. Sensor Actuator B-Chem 2005;105:164–9.